Proceedings of the ASME 2012 31st International Conference on Ocean, Offshore and Arctic Engineering
OMAE2012
July 1-6, 2012, Rio de Janeiro, Brazil

OMAE2012-83997

MPSO DESIGN: PART I – WAVE EXCITATION FORCES AND MOMENTS

Daniel P. Vieira[1]
(daniel.prata@tpn.usp.br)

Edgard B. Malta[1]
(edgard@tpn.usp.br)

Rafael A. Watai[1]
(rafael.watai@tpn.usp.br)

Rodolfo T. Gonçalves[1]
(rodolfo_tg@tpn.usp.br)

André L. C. Fujarra[1]
(afujarra@usp.br)

Kazuo Nishimoto[1]
(knishimo@usp.br)

Allan C. Oliveira[2]
(allan_carre@petrobras.com.br)

[1]TPN – Numerical Offshore Tank
Department of Naval Architecture and Ocean Engineering, Escola Politécnica – University of São Paulo
São Paulo, SP, Brazil

[2]Research and Development Center (CENPES)
PETROBRAS
Rio de Janeiro, RJ, Brazil

ABSTRACT

The MPSO is characterized by the use of hydrodynamics appendages, such as moonpool, beach and skirts, which improve the hydrodynamic behavior of the unit in waves. This type of platform may be designed for different offshore scenarios as, for example: the possibility of oil and gas storage, dry tree completion system and the use of steel catenary risers (SCR). An optimization procedure to choose the geometric dimensions of the MPSO becomes important in order to achieve the optimum hydrodynamic behavior to operate in harsh environmental conditions for each scenario. The optimization procedure might be useful in the preliminary design phases to reduce the verification time of the solution evaluated with model tests; for that reason it is necessary to create a database with experimental results to make the optimization procedure possible. The main idea of the study is to carry out an extensive experimental model test aimed at obtaining the parameters not well predicted using numerical codes. With this intent, the work is subdivided into three parts: Part 1 –Wave Excitation Forces and Moments; Part 2 – Damping and Added Mass Forces and Part 3 – Optimization Process. Results will be presented in different papers. The first one presents the experimental results for captive tests, the second one the experimental results for forced oscillation tests and the last one the methodology to use the experimental results as input in an optimization tool. The first paper presents the methodology in which nondimensional variables based on MPSO geometric characteristics were defined. These variables were related to a fixed moonpool diameter and they were determined in terms of four geometric dimensions: external diameter; height and diameter of the beach and platform draft. As a consequence, 21 different MPSO model geometries could be defined and experimentally tested in order to obtain the wave excitation forces and moments in 6 DOF. The experiments included transient waves so as to better understand the hydrodynamic behavior of the hull, such as, the response amplitude operator (RAO), cancelation points, the beach/bottom/moonpool effects for the different dimensions. The wave forces and moments obtained experimentally were compared to the results of a numerical code based on potential wave theory.

1. INTRODUCTION

The concept of a Monocolumn Production, Storage and Offloading platform (MPSO) has been presented as a solution for offshore applications due to its reduced motions and high stability reserve. Considering its cylindrical geometry, the MPSO resembles spar type platforms as exemplified and presented in Gonçalves et al. (2009). Nevertheless, an important difference between the units is the aspect ratio (L/D, i.e. length/diameter), since spar units have a high value of L/D whereas MPSOs have a small one. Moreover, MPSO may support heavy oil process plants and storage a large amount of oil, since it has a large displacement and water line area.

MPSO is also characterized by the use of hydrodynamics appendages, such as moonpool, beach and skirt, which improve the hydrodynamic behavior of the unit in waves. Due to the large volume of the moonpool and depending on the ratio of its diameter and the unit diameter, it plays an important role in the dynamic behavior acting as a passive absorber; see for instance Cueva et al. (2005), Malta et al (2006), Sphaier et al. (2007) and Torres et al. (2008). Concerning the skirt, its main function it to attenuate the platform motions, by means of the increase of the added mass and viscous damping, as pointed out in Costa et al. (2007), Matsumoto et al. (2008) and Gonçalves et al. (2010).

As observed, several studies involving the MPSO geometry and hydrodynamic appendages were performed aiming at improving its behavior in waves. However, a reliable numerical model for its hydrodynamic assessment, which may be used at the preliminary design stages, is still a challenge. The reasons for this are related to the complexity of modeling the set formed by the hull, moonpool and the skirt, and due to the lack of data that may be used as paradigm for the numerical tools improvements. As a consequence, the concept evaluation is mainly investigated by model scale tests.

An optimization procedure, therefore, becomes an attractive option and might be useful in the preliminary design phases to reduce the verification time of the solution evaluated with model tests.

Hence, the main idea of the study is to carry out an extensive experimental model test aimed at obtaining the parameters not well predicted through the numerical codes. With this intent, the work is subdivided into three parts, being this paper the first one: Part 1 –Wave Excitation Forces and Moments; Part 2 – Damping and Added Mass Forces and Part 3 – Optimization Process.

Experimental tests were carried out in the Hydrodynamic Calibrator of the Numerical Offshore Tank of the University of São Paulo. The tests were performed with different fixed MPSO models exposed to transient waves so as to better understand the hydrodynamic behavior of the hull, such as the exciting forces/moments curves, its cancelation points and the moonpool/beach effects for the different configurations.

The unit model geometry was modified in terms of nondimensional ratios related to the moonpool diameter which was kept fixed during the experiments whereas the external diameter, height and diameter of the beach and draft were changed. Consequently, twenty one different MPSO model geometries could be defined and experimentally tested.

2. EXPERIMENTAL SETUP

Model Design

The main dimensions of a MPSO are: external column diameter (D_c), waterline diameter (D_{wl}), moonpool diameter (D_m), draft (T) and beach height (H_c), as presented in Figure 1.

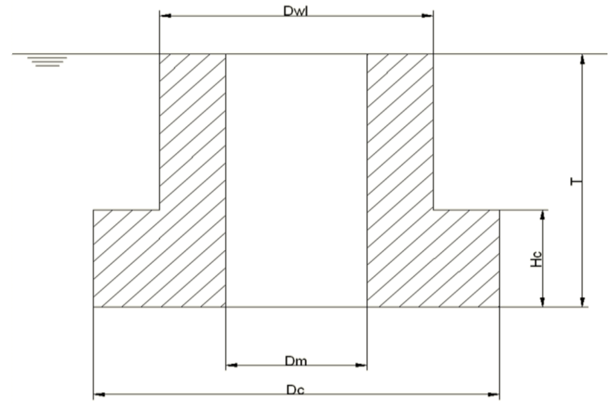

Figure 1 – Main Dimensions of a MPSO.

Torres (2008) showed that the moonpool diameter plays an important role in the wave performance of MPSOs and therefore, was kept constant for all configurations ($D_m = 160mm$). Thus, four nondimensional parameters were defined to characterize the MPSO model: D_c/D_m, D_{wl}/D_m, T/D_m and H_c/D_m. The value ranges of the parameters analyzed were:

Table 1- Nondimensional parameters range of values

Nondimensional	Min	Max
D_c/D_m	2	5.0
D_{wl}/D_m	2	5.0
H_c/D_m	0.5	2.5
T/D_m	0.5	2.5

Models were obtained by stacking 10-mm thick circular PVC plates with eight different external diameters were used ($224mm$, $272mm$, $320mm$, $392mm$, $476mm$, $560mm$, $680mm$ and $800mm$), see Figure 2.

By combining two plates with different external diameters, it was possible to obtain D_c and D_{wl}. The number of stacked plates gives H_c; setting the model on the bridge provides a draft, then a model configuration is defined.

Figure 2- PVC plates used to build the MPSO models.

Table 2 presents a schematic view of the procedure used to vary the parameters and to obtain the several analyzed configurations.

Table 2- Procedure used to obtain the MPSO model configurations.

1st	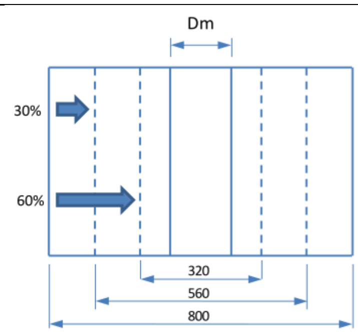
2nd	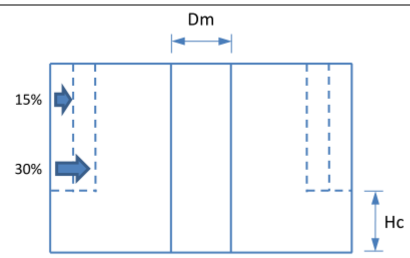
3rd	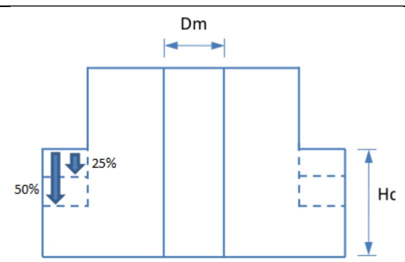

First: only models with $D_c = D_{wl}$, i.e., a cylinder with a moonpool, were considered. The maximum diameter ($800mm$) was reduced by 30% and by 60%. *Second*: Each configuration obtained in the first step had the D_{wl} reduced by 15% and 30% keeping the H_c constant. *Third*: Each configuration obtained in the second step had the H_c reduced by 25% and 50% keeping D_c and D_{wl} constant.

This procedure resulted in 21 configurations which were tested in up to four different drafts. 48 tests were performed overall.

Instrumentation

During the tests three important measures were monitored: the wave force, the incoming wave elevation and the moonpool free surface elevation. Figure 3 shows a schematic view of the experiment layout.

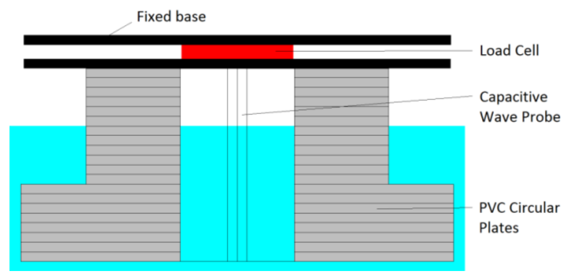

Figure 3 – Schematic view of the experiment layout.

A load cell was attached between a steel plate fixed in the tank bridge and a steel plate fixed on the model. A capacitive wave probe was installed at the moonpool so as to evaluate its elevation, see Figure 4.

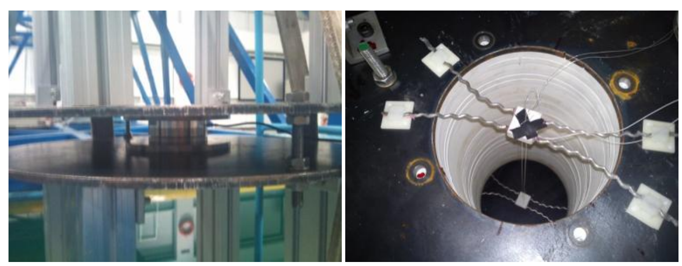

Figure 4 – Setting of load cell (left) and capacitive wave probe (right).

An optical system from Qualysis was used to monitor the incoming wave elevation at the far field, see for instance Fujarra et al. (2009).

3. NUMERICAL MODEL

The numerical predictions were performed using the software WAMIT®, which is a Boundary Element Method code that uses the potential linear wave theory to solve the hydrodynamic problems of diffraction and radiation in the frequency domain, see for instance Wamit Inc. (2006).

Figure 5 presents an example of surface panel meshes designed in MULTISURF® and used as input to the MPSO numerical model in WAMIT®.

Due to the presence of a moonpool, the MPSO is modeled in WAMIT®, as a multibody system (hull plus moonpool). The appropriate way to represent this system is presented in

Matsumoto et al. (2008). This is correct to evaluate the MPSO RAO, but here just the wave forces and moments are evaluated. Once in the experiment the hull is fixed and the moonpool can oscillate freely, and the heave force and moonpool motion are directly coupled, the moonpool motion must be considered in the code for a correct evaluation of heave force.

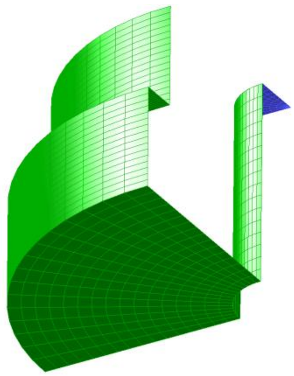

Figure 5 – Surfaces used as input to numerical model. Caption: green – hull submerged surfaces, blue – moonpool free surface.

Firstly, the heave moonpool Response Amplitude Operator (RAO_9) is evaluated as (Subscript 9 refers to moonpool heave, and subscript 3 refers to MPSO heave):

$$RAO_9 = \frac{F_9}{-\omega^2 A_{99} - i\omega B_{99} + C_{99}} \quad (1)$$

where F_9 is the wave exciting force, A_{99} is the added mass, B_{99} is the potential damping, C_{99} the hydrostatic restoring, and ω the wave angular frequency.

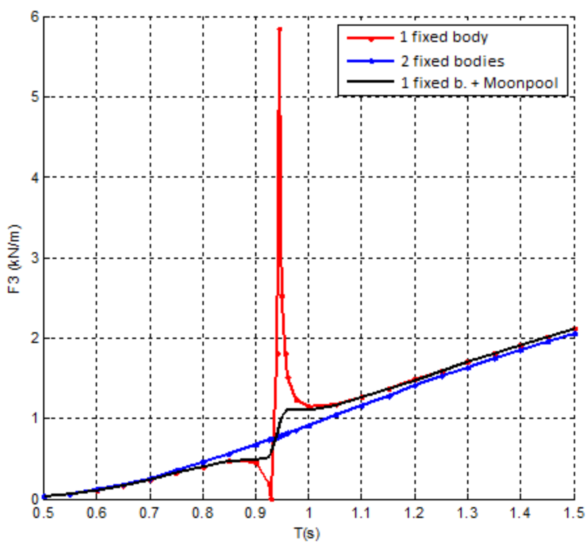

Figure 6 – Comparison among the three different MPSO numerical model.

The corrected heave wave force $(\overline{F_3})$ on the hull is evaluated according:

$$\overline{F_3} = F_3 - (-\omega^2 A_{39} + i\omega B_{39}) RAO_9 \quad (2)$$

where F_3 is the wave force, initially evaluated by the code, and A_{39} and B_{39} are the crossed added mass and potential damping, respectively. Viscous effects of moonpool-hull interaction can be considered adding a external damping on B_{39}. The difference among using the single body model, the model proposed by Matsumoto et al. (2008) and the model proposed here is illustrated in Figure 6.

4. EXTERNAL DAMPING

The external damping was evaluated by two methods. The first method is to adjust the external damping to match the peak of the numerical moonpool RAO to the peak of the experimental moonpool RAO; the damping obtained with this method was denominated ζ_{peak}^{ext}. In the second method, the external damping was adjusted using some points surrounding the moonpool RAO peak, and was denominated ζ_{curve}^{ext}. According to the formulation presented in Chakrabarti (2002) it is possible to write:

$$\zeta(\omega_i) = \sqrt{\left(\frac{RAO_9^{exp}(\omega_i)}{\frac{F_9^{num}(\omega_i)}{C_{99}}}\right)^{-2} - \left(1 - \left(\frac{\omega_i}{\omega_n}\right)^2\right)^2} \quad (3)$$

where $RAO_9^{exp}(\omega_i)$ is the heave moonpool RAO measured at frequency ω_i, $F_9^{num}(\omega_i)$ is the numerical wave force evaluated for frequency ω_i andω_n is the non-damped moonpool resonant frequency. The ζ_{curve}^{ext} is the average of some $\zeta(\omega_i)$. As presented by Torres (2006), the moonpool natural period can be expressed as:

$$\omega_{n_9} = 2\pi\sqrt{\frac{\mathrm{g}}{\mathrm{T} + \mathrm{h_a}}} \quad (4)$$

where $\mathrm{h_a}$ represents the added mass increase due to moonpool, this value can be used to measure the effect of the restriction area at the moonpool entrance.

5. RESULTS

A numerical-experimental comparison is presented in

Figure *7*, Figure 8 and Figure 9 in the Annex.

Figure *7* shows the moonpool RAO, Figure 8 shows the heave wave force and Figure 9 shows the pitch wave moment. Just curves for $T/D_m = 1.5$ and $T/D_m = 2.5$ are presented for simplicity. All presented numerical curves were evaluated using the external damping obtained by the peak method.

The external damping coefficients are presented in Table 3 obtained by the peak and the curve methods. The moonpool external damping varied from 0.4% up to 3.5% by the peak method and from 2% up to 8% by the curve method; also, it can be noticed that the high values were reached at the small drafts.

A comparison can be made with the results presented by Torres (2006), in which the moonpool added mass and damping coefficient were obtained for a series of moonpool restrictions. At the presented study no moonpool restrictions were used and none significant changes in moonpool natural period can be noted. For that reason, considering equation (4), it can be concluded there are no significant changes at h_a value for the same draft and moonpool diameter. Consequently the external dimensions of the hull do not disturb the moonpool added mass.

However, for the moonpool damping, Torres (2006) suggests a curve for the damping coefficient related to the area restriction. For the case with no moonpool restriction and T/D_M close to 0.5, it can be compared with results in Table 3 for T/D_M = 0.5, where the damping coefficients are 3.5% and 1.8% as at Torres (2006) the value is about 3%. This value demonstrates a variation at damping for the same draft but with different external diameters.

Moonpool RAO

It is possible to observe in Figure *7* that in experiments the moonpool natural period was constant for each draft. It is an expected result once the moonpool natural period depends only on draft. For all analyzed cases the greater value was 7.3 m/m. The smallest resonant peak was about 1.3 m/m observed for model number 14 with nondimensional values of D_C/D_M =5 , D_{WL}/D_M= 3.5 and H_C/D_M = 1.

Heave wave force

Comparing both Figure *7* and Figure 8, it is possible to observe a pronounced coupling between moonpool RAO and heave wave forces. Peaks for both curves occur in the same period. Some differences appeared in both drafts presented. In models 11 and 25, the numerical models shows a difference at heave forces that cannot be noticed at the experimental results, for periods up to 1s. In model 8, the experimental results present higher values around 1s periods. Models 13 and 31 did not present the same cancellation points from the numerical model.

Pitch wave moment

The main result for the pitch wave moment at Figure 9 is that the larger is waterline area, the lower is the pitch moment (comparing models with the same external diameter). Model number 2 has the larger waterline area comparing with models 11 and 14, but has the lowest pitch moment. The same result is obtained comparing models 19, 23 and 25 or comparing models 28 and 31.

Comparing models with the same D_{wl}/D_m, for example model 23 with 28 or model 25 with 31, it is observed that the pitch moment is directly related with H_c/D_m, i.e., the larger is the H_c/D_m parameter, the greater is the pitch moment.

Table 3 – External Damping evaluated for all models.

Model	D_C/D_M	D_{WL}/D_M	H_C/D_M	T/D_M	ζ^{ext}_{peak} (%)	ζ^{ext}_{curve} (%)
1	5	5	1	1	1.5	2.18
2	5	5	1.5	1.5	0.9	2.42
3	5	5	2	2	1.2	2.4
4	5	5	2.5	2.5	1.6	4.26
5	5	4.25	2	2.5	1.7	3.33
6	5	3.5	2	2.5	1.7	3.47
7	5	4.25	1.5	2	1.2	2.13
8	5	4.25	1.5	2.5	1.8	3.42
9	5	3.5	1.5	2	1.5	2.64
10	5	3.5	1.5	2.5	2	4.05
11	5	4.25	1	1.5	1.2	2.61
12	5	4.25	1	2	1.1	2.28
13	5	4.25	1	2.5	1.6	3.24
14	5	3.5	1	1.5	2.1	4.93
15	5	3.5	1	2	1.2	2.36
16	5	3.5	1	2.5	1.8	3.68
17	3.5	3.5	0.5	0.5	3.5	7.14
18	3.5	3.5	1	1	1.6	2.93
19	3.5	3.5	1.5	1.5	1.5	3.32
20	3.5	3.5	2	2	2.2	5.87
21	3.5	2.975	1.5	2	1.5	3.22
22	3.5	2.45	1.5	2	1.3	3.33
23	3.5	2.975	1	1.5	1.1	2.86
24	3.5	2.975	1	2	1.3	3.54
25	3.5	2.45	1	1.5	1.1	2.15
26	3.5	2.45	1	2	1	2.8
27	3.5	2.975	0.5	1	1	1.48
28	3.5	2.975	0.5	1.5	1.4	3.53
29	3.5	2.975	0.5	2	1.3	2.83
30	3.5	2.45	0.5	1	0.4	1.31
31	3.5	2.45	0.5	1.5	1.1	2.95
32	3.5	2.45	0.5	2	1	2.77
33	2	2	0.5	0.5	1.8	7.58
34	2	2	0.75	0.75	1.4	4.39
35	2	2	1	1	1.3	3.1
36	2	2	1.25	1.25	1.3	3.74
37	2	1.7	1	1.25	1.5	3.76
38	2	1.4	1	1.25	1.2	4.25
39	2	1.7	0.75	1	1.2	2.53
40	2	1.7	0.75	1.25	1.5	3.7
41	2	1.4	0.75	1	1.3	2.46
42	2	1.4	0.75	1.25	1.5	2.65
43	2	1.7	0.5	0.75	2	5.96
44	2	1.7	0.5	1	1.4	2.97
45	2	1.7	0.5	1.25	1.4	3.74
46	2	1.4	0.5	0.75	1.5	6.71
47	2	1.4	0.5	1	1.3	2.31
48	2	1.4	0.5	1.25	1.5	4.39

6. GENERAL CONCLUSIONS

The results were analyzed for the external damping, the moonpool response amplitude operator, the heave wave force and the pitch wave moment. These excitation forces could be an input for the design of monocolumn platforms. The comparison between experimental and numerical data gives the information about how the numerical results are reliable for an optimization process.

About the moonpool response, the values must be considered in the design of MPSO air gap. Although the moonpool is used to minimize the heave motion, the observed large amplitudes can cause serious damage to the structure below the deck. It was noted that the moonpool natural period is a function of the moonpool diameter and draft. However, the external damping should consider the external dimension in order to obtain better levels of moonpool response. In case of moonpool restrictions, these parameters also affect added mass and damping as presented by Torres (2006).

Future Work

As a future activity, a forced motion oscillation test will be performed in order to obtain the heave and pitch added mass, radiation damping and external damping coefficients. These results can be used in a better motion evaluation of monocolumn platform designs.

NOMENCLATURE

ω	Angular frequency
ω_n	Natural angular frequency
ζ_{peak}^{ext}	External MPSO-moonpool damping evaluated by peak method
ζ_{curve}^{ext}	External MPSO-moonpool damping evaluated by curve method
A_{39}	MPSO-Moonpool crossed heave added mass
A_{99}	Moonpool heave added mass
B_{99}	Moonpool heave potential damping
B_{39}	MPSO-Moonpool crossed heave potential damping
C_{99}	Moonpool heave hydrodtatic restoring
D	Characteristic diameter of the platform
D_c	External MPSO Diameter
D_m	Moonpool Diameter
D_{wl}	Waterline Diameter
F_3	MPSO heave wave force
$\overline{F_3}$	MPSO corrected heave wave force
F_9	Moonpool heave wave force
F_9^{num}	Moonpool heave wave force evaluated numerically
h_a	Moonpool added mass increasing
RAO_9	Moonpool heave response amplitude operator
RAO_9^{exp}	Moonpool heave response amplitude operator measured in experiment
T	MPSO draft

ACKNOWLEDGMENTS

The authors thank PETROBRAS for their help in conducting the research. The first author thanks the National Petroleum Agency (ANP) for the financial support.

REFERENCES

1. Chakrabarti, S. (2002). *The Theory and Pratice of Hydrodynamics an Vibration.* World Scientific Publishing Co.

2. Costa, A. P. S., Matter, G. B., Masetti, I. Q., Barreira, R., & Sphaier, S. H. (2007). Effect of Skirts an Beaches on the Behavior of a Monocolumn Structure in Waves. *26th International Conference on Offshore Mechanics and Artic Engineering. OMAE2007-29024* .

3. Cueva, M. F., Fujarra, A. L. C., & Nishimoto, K. (2006). Vortex Induced Motions: Model Testing of a Monocolumn Floater. *25th International Conference on Offshore Mechanics and Artic Engineering. OMAE2006-92167* .

4. Fujarra, A. L., Gonçalves, R. T., Fonseca, R. P., Siewert, K., & Martins, J. A. (2009). Optical Motion Capture as a Techinique for Measuring the Water Wave Elevation. *4th International Workshop pn Applied Offshore Hydrodynamics (IWAOH).* Rio de Janeiro, RJ, Brazil.

5. Gonçalves, R. T., Rosetti, G. F., Matsumoto, F. T., Malta, E. B., Rosetti, G. F., Fujarra, A. L. C., & Nishimoto, K. (2009). Evolution of the MPSO (monocolumn production, storage and offloading system). *Marine Systems & Ocean Technology*. Vol. 5, No. 1, PP. 43-51. December 2009/June 2010.

6. Gonçalves, R. T., Matsumoto, F. T., Malta, E. B., Medeiros, H. F., & Nishimoto, K. (2010). Conceptual Design of Monocolumn Production and Storage With Dry Tree Capability. *Journal of Offshore Mechanics and Arctic Engineering*, v. 132, p. 041301-1-041301-12.

7. Malta, E. B., Cueva, M. F., & Nishimoto, K. (2006). Numerical Moonpool Modeling. *25th International Conference on Offshore Mechanics and Artic Engineering. OMAE2006-92456* .

8. Matsumoto, F. T., Gonçalves, R. T., & Malta, E. B. (2008). The Influence at Vertical First Order Motions Using Appendages in a Monocolumn Platform. *27th International Conference on Offshore Mechanics and artic Engineering. OMAE2008-57410* .

9. Sphaier, S. H., Torres, F. G., Masetti, I. Q., Costa, A. P., & Levi, C. (2007). Monocolumn Behavior in Waves: Experimental Analysis. *Ocean Engineering* , pp. 1724-1733.

10. Torres, F. G., Nishimoto, K., Malta, E. B., & Masetti, I. Q. (2008). The numerical Model of Moonpool as a Vertical Motion Absorbing Device in the Monocolumn Type Platform. *20th Ocean Engineering Symposium*.

11. Torres, F. G., (2006). “Estudo do moonpool como sistema de minimização de movimento de uma plataforma do tipo monocoluna”. Master Thesis at University of São Paulo.

12. Wamit Inc., (2006). “Wamit User Manual, Versions 6.4 and 6.4PC”. Massachussets Institute of Technology.

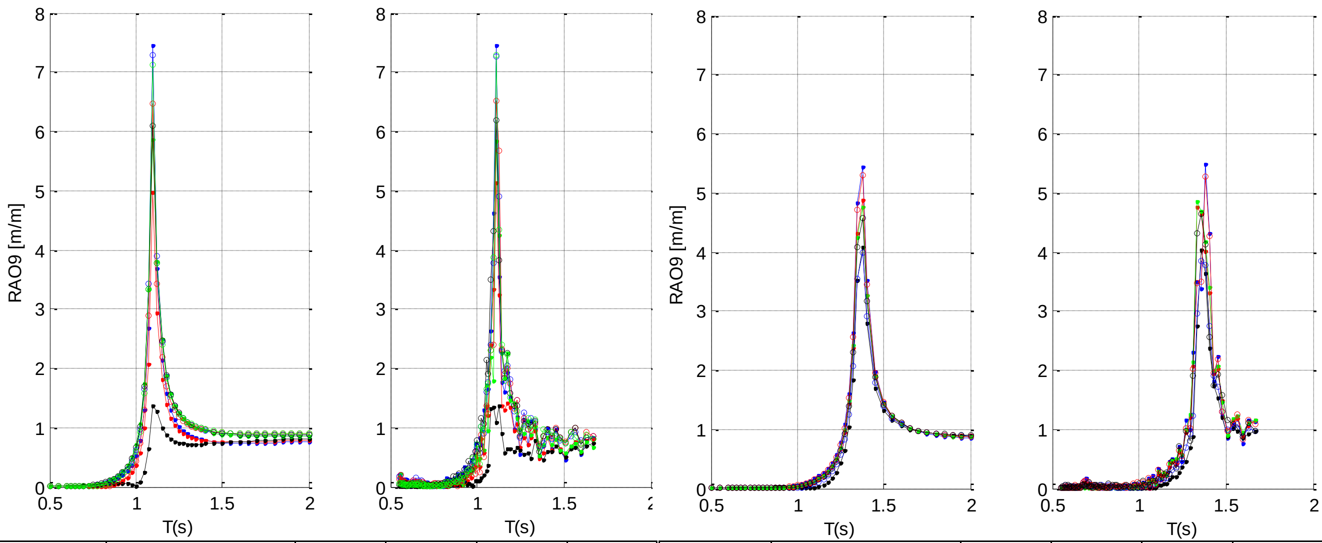

Legend	Sketch	Model	D_C/D_M	D_{WL}/D_M	H_C/D_M	Legend	Sketch	Model	D_C/D_M	D_{WL}/D_M	H_C/D_M
		2	5	5	1.5			4	5	5	2.5
		11	5	4.25	1			5	5	4.25	2
		14	5	3.5	1			6	5	3.5	2
		19	3.5	3.5	1.5			8	5	4.25	1.5
		23	3.5	2.975	1			10	5	3.5	1.5
		25	3.5	2.45	1			13	5	4.25	1
		28	3.5	2.975	0.5			16	5	3.5	1
		31	3.5	2.45	0.5						

Figure 7 – Moonpool RAO for $T/D_m = 1.5$ (left) and $T/D_m = 2.5$ (right).

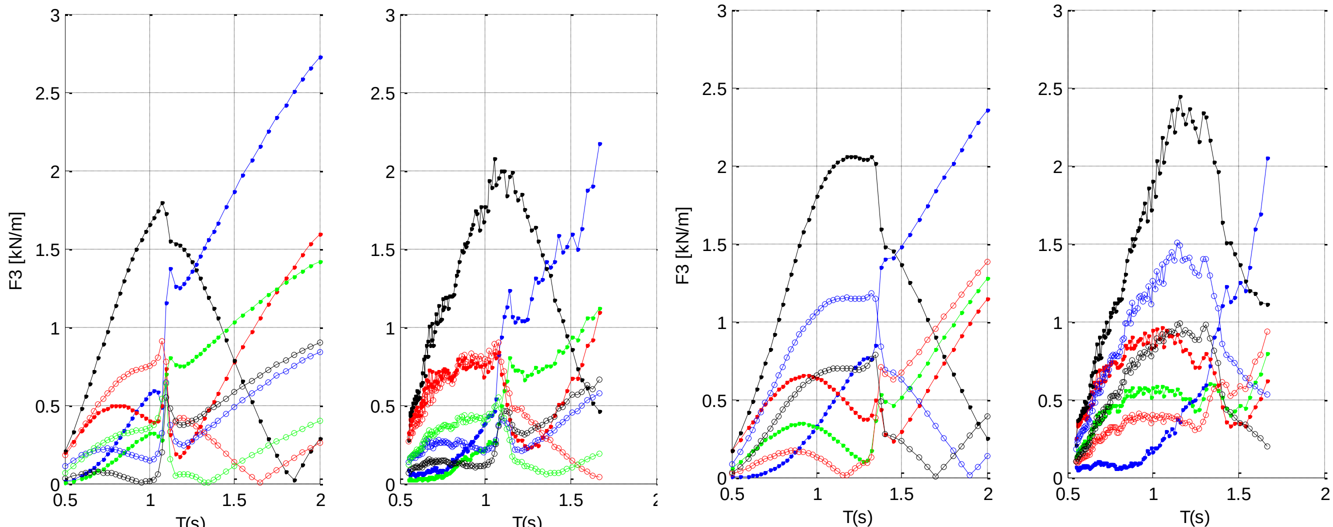

Legend	Sketch	Model	D_C/D_M	D_{WL}/D_M	H_C/D_M
	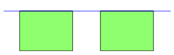	2	5	5	1.5
	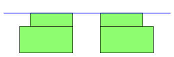	11	5	4.25	1
	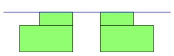	14	5	3.5	1
	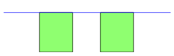	19	3.5	3.5	1.5
	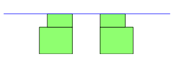	23	3.5	2.975	1
	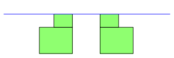	25	3.5	2.45	1
	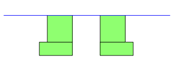	28	3.5	2.975	0.5
	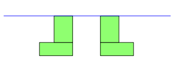	31	3.5	2.45	0.5

Legend	Sketch	Model	D_C/D_M	D_{WL}/D_M	H_C/D_M
	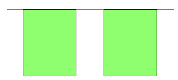	4	5	5	2.5
	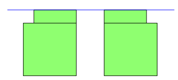	5	5	4.25	2
	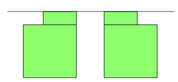	6	5	3.5	2
	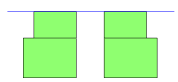	8	5	4.25	1.5
	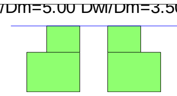	10	5	3.5	1.5
	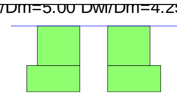	13	5	4.25	1
	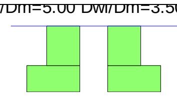	16	5	3.5	1

Figure 8 – Heave force on hull for T/D_m = 1.5 (left) and T/D_m = 2.5 (right).

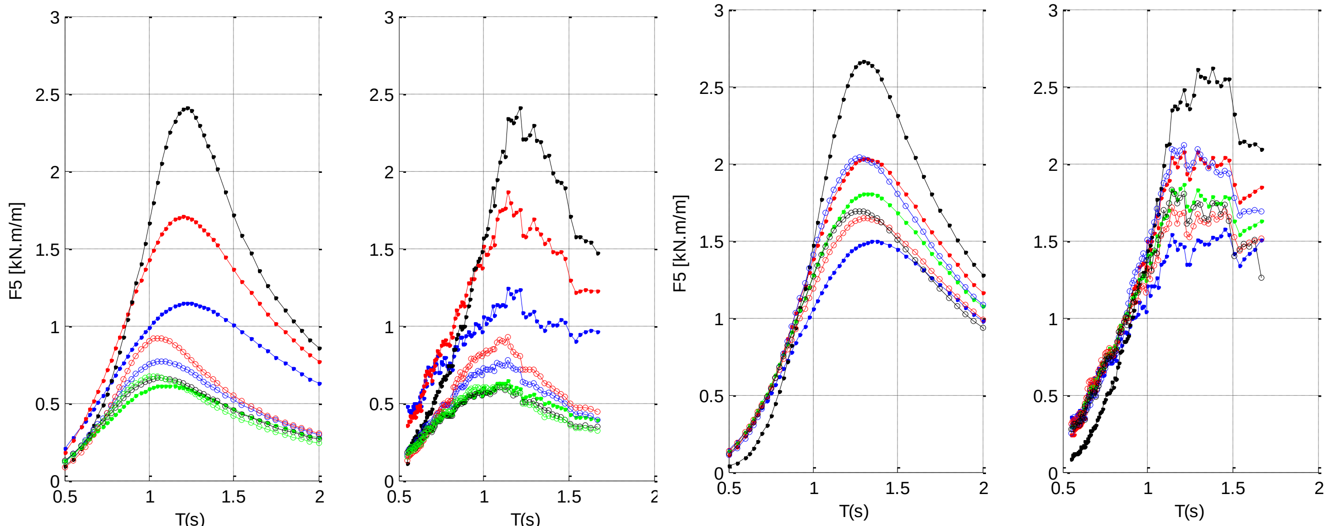

Legend	Sketch	Model	D_C/D_M	D_{WL}/D_M	H_C/D_M	Legend	Sketch	Model	D_C/D_M	D_{WL}/D_M	H_C/D_M
	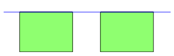	2	5	5	1.5		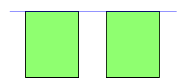	4	5	5	2.5
	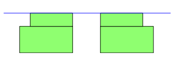	11	5	4.25	1		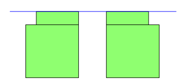	5	5	4.25	2
	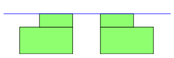	14	5	3.5	1		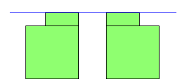	6	5	3.5	2
	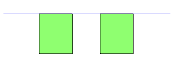	19	3.5	3.5	1.5		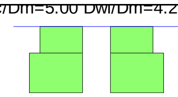	8	5	4.25	1.5
	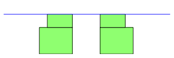	23	3.5	2.975	1		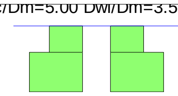	10	5	3.5	1.5
	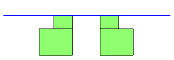	25	3.5	2.45	1		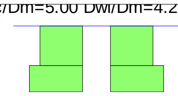	13	5	4.25	1
	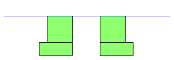	28	3.5	2.975	0.5		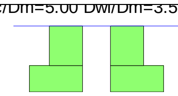	16	5	3.5	1
	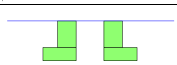	31	3.5	2.45	0.5						

Figure 9 - Pitch moment on hull for T/D_m = 1.5 (left) and T/D_m = 2.5 (right).